PARIS 2017

Theory for Marchenko imaging of marine seismic data with free surface multiple elimination

Evert Slob and Kees Wapenaar
Delft University of Technology

Summary

The theory of data-driven true amplitude migration is presented for multicomponent marine seismic data. The Marchenko scheme is adapted to account for the ghost, free surface and internal multiple effects and works without the need to know the source wavelet. A true amplitude image is formed from the obtained focusing functions without ghost effects and artefacts from free surface and internal multiples. The resulting reflectivity at image times can be input for a final step of full waveform inversion. The numerical example shows the effectiveness of the method in a simple 1D problem.

Introduction

Combining free surface multiple elimination and internal multiple elimination is an ongoing research effort. Examples of doing this using the inverse scattering series can be found in Weglein et al. (2003) and for land data with the Marchenko method can be found in Singh et al. (2015, 2017). In this abstract we present a Marchenko scheme for marine seismic data where we assume the wavefield is recorded such that vertical particle velocity data is properly sampled and can be obtained in separate up- and downgoing components. We show how this scheme accounts for the ghost effects and deals with free surface and internal multiples such that an image is obtained without artefacts coming form these effects in the data. We also show how this scheme can be set up such that the source wavelet does not need to be known. We illustrate the presented method with a 1D numerical example to show the effectiveness of the scheme in 1D.

Representation for vertical particle velocity data

The configuration consists of a heterogeneous half space below a pressure free surface at $z = 0$. The source is located below the surface, $z_s > 0$, and receivers are assumed to be placed below the source, $z_r > z_s$. Outside the source depth level the acoustic pressure, p, satisfies the homogeneous wave equation given by

$$\rho\nabla\cdot(\rho^{-1}\nabla p)+\frac{1}{c^2}\partial_t^2 p=0, \tag{1}$$

where $\rho(\mathbf{x}), c(\mathbf{x})$ denote the position dependent mass density and wave velocity. Frequency domain expressions are obtained by replacing the time-derivative by the factor $\mathrm{j}\omega$ and frequency dependent quantities are indicated with a diacritical hat, e.g., the acoustic pressure is denoted $\hat{p}$. The particle velocity is related to the pressure as $\hat{\mathbf{v}} = -(\mathrm{j}\omega\rho)^{-1}\nabla\hat{p}$. For these field quantities the reciprocity theorems of the time-convolution and time-correlation types can be used to obtain relations between the fields in two different states, labeled A and B. We apply reciprocity to a domain that has two horizontal boundaries of infinite extent at depth levels z_r and z_i, both located below the source depth level and $z_i > z_r$. Between the two depth levels we take the medium in both states the same and no sources exist inside the domain or on the boundaries. In that case the reciprocity relations are given by (Wapenaar and Grimbergen, 1996)

$$\int_{\partial\mathbb{D}_r}[\hat{p}_A^+(\mathbf{x}_r)\hat{v}_{z,B}^-(\mathbf{x}_r)+\hat{p}_A^-(\mathbf{x}_r)\hat{v}_{z,B}^+(\mathbf{x}_r)]\mathrm{d}^2\mathbf{x}_r=-\int_{\partial\mathbb{D}_i}[\hat{v}_{z,A}^+(\mathbf{x}_i)\hat{p}_B^-(\mathbf{x}_i)+\hat{v}_{z,A}^-(\mathbf{x}_i)\hat{p}_B^+(\mathbf{x}_i)]\mathrm{d}^2\mathbf{x}_i, \tag{2}$$

$$\int_{\partial\mathbb{D}_r}[(\hat{p}_A^+(\mathbf{x}_r))^*\hat{v}_{z,B}^+(\mathbf{x}_r)+(\hat{p}_A^-(\mathbf{x}_r))^*\hat{v}_{z,B}^-(\mathbf{x}_r)]\mathrm{d}^2\mathbf{x}_r=\int_{\partial\mathbb{D}_i}[(\hat{v}_{z,A}^+(\mathbf{x}_i))^*\hat{p}_B^+(\mathbf{x}_i)+(\hat{v}_{z,A}^-(\mathbf{x}_i))^*\hat{p}_B^-(\mathbf{x}_i)]\mathrm{d}^2\mathbf{x}_i, \tag{3}$$

where it is assumed that the density and velocity at the depth level z_i are continuously differentiable in horizontal direction, while for equation (3) an additional approximation is made by ignoring evanescent waves at both depth levels, as described in Appendix B in Wapenaar and Berkhout (1989). The wavefields are split in up- and downgoing components indicated by minus- and plus-signs in superscript, e.g., the acoustic pressure has an upgoing component $\hat{p}^-$ and a downgoing component $\hat{p}^+$.

In state A we take the medium between z_r and z_i the same as the actual medium, whereas above the receiver level z_r and below the focusing level z_i it is homogeneous with the medium parameters of the actual medium at those depth levels. In this reduced medium we define an acoustic pressure related focusing wavefield, $\hat{f}_1(\mathbf{x},\mathbf{x}_i')$, that focuses at a point $\mathbf{x}_i'$ at depth level z_i. Hence at the receiver level we have $\hat{p}_A^{\pm}(\mathbf{x}_r)=\hat{f}_1^{\pm}(\mathbf{x}_r,\mathbf{x}_i')$. At the focusing level we express the focusing particle velocity field in up- and downgoing pressure focusing field components as

$$\hat{v}_{z,A}(\mathbf{x}_i)=-(\mathrm{j}\omega\rho)^{-1}[\partial_z\hat{f}_1^+(\mathbf{x}_i,\mathbf{x}_i')+\partial_z\hat{f}_1^-(\mathbf{x}_i,\mathbf{x}_i')]. \tag{4}$$

The focusing condition is given by

$$\partial_z\hat{f}_1^+(\mathbf{x}_i,\mathbf{x}_i')=-\frac{1}{2}\mathrm{i}\omega\rho\,\delta(\mathbf{x}_T-\mathbf{x}_T'), \qquad \text{and} \qquad \partial_z\hat{f}_1^-(\mathbf{x}_i,\mathbf{x}_i')=0, \tag{5}$$

which implies that the wavefield focuses in $\mathbf{x}_i = \mathbf{x}_i'$ after which it propagates downwards as a diverging wavefield and there is no upgoing wavefield at and below depth level z_i. In state B we take the actual medium with a free surface and possible other heterogeneities above the receiver level z_r. At the receiver level we assume the up-and downgoing components of the vertical component of the particle velocity are obtained from measurements. This can be achieved using over-under pressure field data or when both pressure and vertical component of the particle velocity data are acquired in streamer data (Amundsen, 2001), or when mutlicomponent OBC data is available (Amundsen et al., 2001). At depth level z_i we write the pressure in its up- and downgoing components as

$$\hat{p}_B(\mathbf{x}_i) = \hat{p}^+(\mathbf{x}_i,\mathbf{x}_s) + \hat{p}^-(\mathbf{x}_i,\mathbf{x}_s), \tag{6}$$

where the source position $\mathbf{x}_s$ is explicitly given.

Substitution of these choices of the wavefields in equations (2) and (3) gives

$$\hat{p}^-(\mathbf{x}_i,\mathbf{x}_s) = -2\int_{\partial\mathbb{D}_r} [\hat{f}_1^+(\mathbf{x}_r,\mathbf{x}_i)\hat{v}_z^-(\mathbf{x}_r,\mathbf{x}_s) + \hat{f}_1^-(\mathbf{x}_r)\hat{v}_z^+(\mathbf{x}_r,\mathbf{x}_s)]\mathrm{d}^2\mathbf{x}_r, \tag{7}$$

$$\hat{p}^+(\mathbf{x}_i,\mathbf{x}_s) = 2\int_{\partial\mathbb{D}_r} [(\hat{f}_1^+(\mathbf{x}_r,\mathbf{x}_i))^*\hat{v}_z^+(\mathbf{x}_r,\mathbf{x}_s) + (\hat{f}_1^-(\mathbf{x}_r,\mathbf{x}_i))^*\hat{v}_z^-(\mathbf{x}_r,\mathbf{x}_s)]\mathrm{d}^2\mathbf{x}_r. \tag{8}$$

These equations relate the upgoing and downgoing pressure wavefield at a virtual receiver located in the subsurface at $\mathbf{x}_i$ and generated by a source at $\mathbf{x}_s$ in terms of integrals over all receiver locations of the decomposed data $\hat{v}_z^\pm$ and the decomposed focusing wavefield $\hat{f}_1^\pm$. Note that the required wavefield has only been decomposed in up-and downgoing parts and both components contain ghost events and surface related multiples as well as the source signature. All these effects will still be present in the pressure field at the focusing level. In the time domain equations (7) and (8) are given by

$$p^-(\mathbf{x}_i,\mathbf{x}_s,t) = -2\int_{\partial\mathbb{D}_r}\int_{t'=-\infty}^{t} \left[f_1^+(\mathbf{x}_r,\mathbf{x}_i,t')v_z^-(\mathbf{x}_r,\mathbf{x}_s,t-t') + f_1^-(\mathbf{x}_r,\mathbf{x}_i,t')v_z^+(\mathbf{x}_r,\mathbf{x}_s,t-t')\right]\mathrm{d}t'\mathrm{d}\mathbf{x}_r, \tag{9}$$

$$p^+(\mathbf{x}_i,\mathbf{x}_s,t) = 2\int_{\partial\mathbb{D}_r}\int_{t'=-\infty}^{t} \left[f_1^+(\mathbf{x}_r,\mathbf{x}_i,-t')v_z^+(\mathbf{x}_r,\mathbf{x}_s,t-t') + f_1^-(\mathbf{x}_r,\mathbf{x}_i,-t')v_z^-(\mathbf{x}_r,\mathbf{x}_s,t-t')\right]\mathrm{d}t'\mathrm{d}\mathbf{x}_r, \tag{10}$$

where causality of the measured wavefield defines the upper integration limit of the time integrals. The left-hand sides of equations (9) and (10) are the up- and downgoing acoustic pressure fields at a point $\mathbf{x}_i$ in the subsurface and generated by a source in $\mathbf{x}_s$. We let the source be excited at $t = 0$ and the first arrival is recorded in $\mathbf{x}_i$ at $t = t_d(\mathbf{x}_i,\mathbf{x}_s)$. This implies that for $t < t_d(\mathbf{x}_i,\mathbf{x}_s)$ both left-hand sides are zero. Because the focusing wavefield collapses its vertical component of the particle velocity to a delta function at $\mathbf{x}_i$ and $t = 0$, it is a non-causal wavefield at the receiver level that starts to exist at $t = -t_d(\mathbf{x}_i,\mathbf{x}_r)$ and for similar reason it ceases to exist for $t > t_d(\mathbf{x}_i,\mathbf{x}_r)$. Evaluating equations (9) and (10) for $t < t_d(\mathbf{x}_i,\mathbf{x}_r)$ we end up with

$$\int_{\partial\mathbb{D}_r}\int_{t'=-t_d}^{t} f_1^+(\mathbf{x}_r,\mathbf{x}_i,t')v_z^-(\mathbf{x}_r,\mathbf{x}_s,t-t')\mathrm{d}t'\mathrm{d}\mathbf{x}_r = -\int_{\partial\mathbb{D}_r}\int_{t'=-t_d}^{t} f_1^-(\mathbf{x}_r,\mathbf{x}_i,t')v_z^+(\mathbf{x}_r,\mathbf{x}_s,t-t')\mathrm{d}t'\mathrm{d}\mathbf{x}_r, \tag{11}$$

$$\int_{\partial\mathbb{D}_r}\int_{t'=-t_d}^{t} f_1^-(\mathbf{x}_r,\mathbf{x}_i,-t')v_z^-(\mathbf{x}_r,\mathbf{x}_s,t-t')\mathrm{d}t'\mathrm{d}\mathbf{x}_r = -\int_{\partial\mathbb{D}_r}\int_{t'=-t_d}^{t} f_1^+(\mathbf{x}_r,\mathbf{x}_i,-t')v_z^+(\mathbf{x}_r,\mathbf{x}_s,t-t')\mathrm{d}t'\mathrm{d}\mathbf{x}_r, \tag{12}$$

where $t_d = t_d(\mathbf{x}_i,\mathbf{x}_r)$. Equations (11) and (12) are two coupled 3D Marchenko-type equations from which $f_1^\pm(\mathbf{x}_r,\mathbf{x}_i,t)$ can be solved in the interval $-t_d(\mathbf{x}_i,\mathbf{x}_r) \le t < t_d(\mathbf{x}_i,\mathbf{x}_r)$. At the time instant $t = t_d(\mathbf{x}_i,\mathbf{x}_s)$ the downgoing pressure in equation (10) is non-zero and that means that $f_1^+(\mathbf{x}_r,\mathbf{x}_i,t)$ can be non-zero, whereas $f_1^-(\mathbf{x}_r,\mathbf{x}_i,t) = 0$, at $t = \pm t_d(\mathbf{x}_i,\mathbf{x}_r)$. Because we exclude the time instant $t = t_d(\mathbf{x}_i,\mathbf{x}_r)$ we need an initial estimate for the downgoing part of the focusing wavefields at $t = t_d(\mathbf{x}_i,\mathbf{x}_r)$. To focus the field at depth requires to send in the inverse of the transmission response. Hence we can write the downgoing part of the focusing wavefield as

$$f_1^+(\mathbf{x}_r,\mathbf{x}_i,t) = f_{1d}^+(\mathbf{x}_r,\mathbf{x}_i,t) + f_{1m}^+(\mathbf{x}_r,\mathbf{x}_i,t), \tag{13}$$

where $f_{1d}^{+}(\mathbf{x}_r,\mathbf{x}_i,t)$ denotes the first arrival of the inverse of the transmission response between $\mathbf{x}_r$ and $\mathbf{x}_i$ and $f_{1m}^{+}(\mathbf{x}_r,\mathbf{x}_i,t)$ represents the coda following the first arrival. Because we do not have a single delta-like event in the measured data we cannot use the usual iterative scheme (Slob et al., 2014; Wapenaar et al., 2014) and must resort to other methods such as the conjugate gradient iterative method or matrix inversion. This leads to the following operator equation

$$\mathscr{L}_{11}f_{1m}^{+}+\mathscr{L}_{12}f_{1}^{-}=d_1, \tag{14}$$
$$\mathscr{L}_{21}f_{1m}^{+}+\mathscr{L}_{22}f_{1}^{-}=d_2, \tag{15}$$

with

$$\mathscr{L}_{11}f_{1m}^{+}=\int_{\partial\mathbb{D}_r}\int_{t'=-t_d}^{t} v_z^{-}(\mathbf{x}_r,\mathbf{x}_s,t-t')f_{1m}^{+}(\mathbf{x}_r,\mathbf{x}_i,t')\mathrm{d}t'\mathrm{d}\mathbf{x}_r, \tag{16}$$
$$\mathscr{L}_{12}f_{1}^{-}=\int_{\partial\mathbb{D}_r}\int_{t'=-t_d}^{t} v_z^{+}(\mathbf{x}_r,\mathbf{x}_s,t-t')f_{1}^{-}(\mathbf{x}_r,\mathbf{x}_i,t')\mathrm{d}t'\mathrm{d}\mathbf{x}_r, \tag{17}$$
$$\mathscr{L}_{21}f_{1m}^{+}=\int_{\partial\mathbb{D}_r}\int_{t'=-t}^{t_d} v_z^{+}(\mathbf{x}_r,\mathbf{x}_s,t+t')f_{1m}^{+}(\mathbf{x}_r,\mathbf{x}_i,t')\mathrm{d}t'\mathrm{d}\mathbf{x}_r, \tag{18}$$
$$\mathscr{L}_{22}f_{1}^{-}=\int_{\partial\mathbb{D}_r}\int_{t'=-t}^{t_d} v_z^{-}(\mathbf{x}_r,\mathbf{x}_s,t+t')f_{1}^{-}(\mathbf{x}_r,\mathbf{x}_i,t')\mathrm{d}t'\mathrm{d}\mathbf{x}_r, \tag{19}$$

and

$$d_1=-\int_{\partial\mathbb{D}_r}\int_{t'=-t_d}^{t} v_z^{-}(\mathbf{x}_r,\mathbf{x}_s,t-t')f_{1d}^{+}(\mathbf{x}_r,\mathbf{x}_i,t')\mathrm{d}t'\mathrm{d}\mathbf{x}_r, \tag{20}$$
$$d_2=-\int_{\partial\mathbb{D}_r}\int_{t'=-t_d}^{t} v_z^{+}(\mathbf{x}_r,\mathbf{x}_s,t-t')f_{1d}^{+}(\mathbf{x}_r,\mathbf{x}_i,-t')\mathrm{d}t'\mathrm{d}\mathbf{x}_r. \tag{21}$$

These equations can be solved by unconditional iterative methods, such as the CG method, or through matrix inversion techniques. An example of sparse inversion can be found in Staring et al. (2017).

Numerical example

To illustrate the method we use a one-dimensional model. The model consists of a layered medium with 10 reflecting interfaces below the source and receiver and a free surface above them at z=0. The source and receiver depths are $z_s = 10$ m and $z^r = 25$ m. The layered model is given in Table 1. The first layer is the water layer in which the source and receivers are located. The source emits an upgoing and a downgoing normal incidence plane Ricker wavelet with 60 Hz center frequency. The vertical component of the particle velocity is computed separately in its downgoing and upgoing parts as input for the Marchenko equations. We solve equations (14) and (15) by matrix inversion for all image times and create an image directly from f_1^- as presented in Slob et al. (2014).

Table 1 *density and velocity model.*

d (m)	75	117	99	85	111	75	123	151	163	221	∞
ρ (kg/m^3)	1000	2250	1750	1430	1750	1930	1500	2110	2110	2250	2300
c (m/s)	1500	1900	2100	1700	2100	2300	2100	2100	2500	2750	2900

The left plot of Figure 1 shows the downging (black solid line) and upgoing (red dashed line) vertical component of the particle velocity including the ghost, free surface and internal multiple effects. The up- and downgoing parts are assumed to be available separately as input for the scheme. The right plot of Figure 1 shows the ideal image at image time in the black solid line and the obtained image from the presented Marchenko scheme in the red dashed line. It can be seen that the ghost effect is absent from the image and no artefacts occur from the free surface or internal multiples.

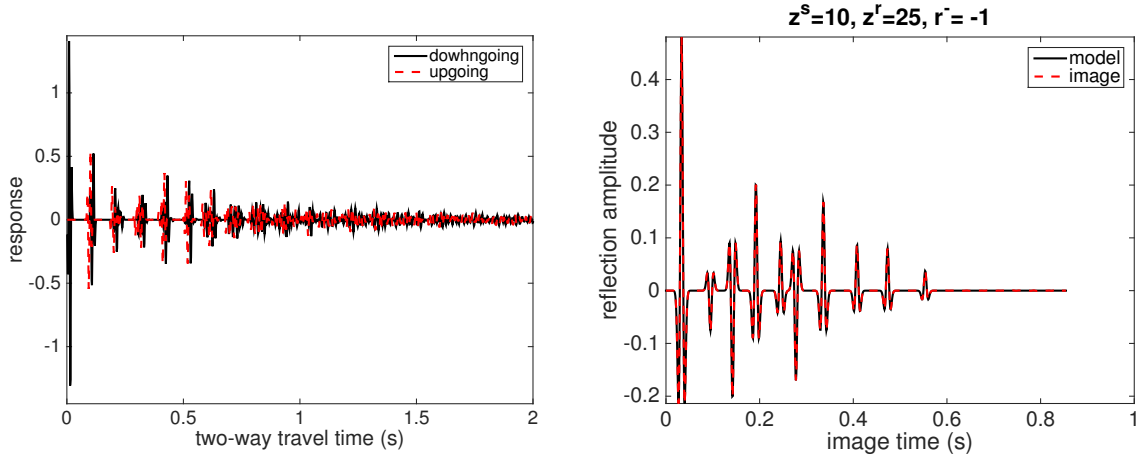

Figure 1 *Left: The vertical particle velocity in its downgoing (black solid line) and upgoing (red dashed line) components measured 25 m and generated by a source 10 m below the free surface over a model with ten reflecting boundaries. Right: the obtained image (red dashed line) and the ideal image convolved with Ricker wavelet (black solid line).*

Conclusions

We have presented the theory for a scheme that could work on marine seismic data in case the data can be decomposed into the up- and downgoing components of the vertical particle velocity at the receiving depth level. These data would still include ghost effects as well as free surface and internal multiples. We have formulated the scheme such that the source wavelet does not need to be known. The focusing wavefield is obtained in separated up- and downgoing components from which the true amplitude image can be formed at the correct image time. The numerical example showed that the scheme performs well on ideal 1D model data.

References

Amundsen, L. [2001] Elimination of free-surface related multiples without need of the source wavelet. *Geophysics*, **66**(1), 327–341.

Amundsen, L., Ikelle, L.T. and Berg, L.E. [2001] Multidimensional signature deconvolution and free-surface multiple elimination of marine multicomponent ocean-bottom seismic. *Geophysics*, **66**(5), 1594–1604.

Singh, S., Snieder, R., Behura, J., van der Neut, J., Wapenaar, K. and Slob, E.C. [2015] Marchenko imaging: Imaging with primaries, internal multiples, and free-surface multiples. *Geophysics*, **80**(5), S165–S174.

Singh, S., Snieder, R., van der Neut, J., Thorbecke, J., Slob, E.C. and Wapenaar, K. [2017] Accounting for free-surface multiples in Marchenko imaging. *Geophysics*, **82**(1), R19–R30.

Slob, E., Wapenaar, K., Broggini, F. and Snieder, R. [2014] Seismic reflector imaging using internal multiples with Marchenko-type equations. *Geophysics*, **79**(2), S63–S76.

Staring, M., van der Neut, J., Grobbe, N. and Wapenaar, K. [2017] Sparse inversion for solving the coupled Marchenko equations including free-surface multiples. In: *Paris 2017*. this meeting.

Wapenaar, C.P.A. and Berkhout, A.J. [1989] *Elastic wave field extrapolation: Redatuming of single- and multi- component seismic data*. Advances in Exploration Geophysics. Elsevier Science Publishers.

Wapenaar, C.P.A. and Grimbergen, J.L.T. [1996] Reciprocity theorems for one-way wavefields. *Geophysical Journal International*, **127**(1), 169–177.

Wapenaar, K., Thorbecke, J., van der Neut, J., Broggini, F., Slob, E. and Snieder, R. [2014] Marchenko Imaging. *Geophysics*, **79**(3), WA39–WA57.

Weglein, A.B., Araújo, F.V., Carvalho, P.M., Stolt, R.H., Matson, K.H., Coates, R.T., Corrigan, D., Foster, D.J., Shaw, S.A. and Zhang, H. [2003] Inverse scattering series and seismic exploratoin. *Inverse problems*, **19**(6), R27–R83.